

Published in Solar Energy Materials & Solar Cells **92**, (5), 537–542, (2008) © by 2007 Elsevier B.V. All rights reserved..
DOI 10.1016/j.solmat.2007.11.009

Single-step preparation of inverse opal titania films by the doctor blade technique

G. Ruani^{a*}, C. Ancora^a, F. Corticelli^b, C. Dionigi^a, and C. Rossi^a

^aIstituto per lo Studio dei Materiali Nanostrutturati ISMN-CNR, via Gobetti, 101 – I-40129 Bologna - Italy

^bIstituto per la Microelettronica e Microsistemi IMM-CNR, via Gobetti, 101 – I-40129 Bologna – Italy

Abstract:

The difficulty to infiltrate solid-state hole semiconductors within micron-thick porous titania films is one of the major limiting factors for the achievement of efficient solid state dye-sensitized solar cells. It was already shown that through the ordered interconnected pores of an inverse opal, the large surface area of several microns thick titania film can be easily decorated with a dye and filled with a solid-state hole semiconductor. In this paper we show that ordered inverse opal mesoporous thick films of TiO₂ with these characteristics can be obtained by using a slurry of monodispersed polystyrene spheres and a titania-lactate precursor deposited by the doctor blade technique. The mechanism of formation of the inverse opal is also discussed.

Keywords: TiO₂ inverse opals, dye-sensitized solar cell, self-assembling, Raman scattering, hydrophobic attraction forces.

*Corresponding author:

Giampiero Ruani, ISMN-CNR, via Gobetti, 101 – I-40129 Bologna – Italy

E-mail address: g.ruani@bo.ismn.cnr.it

G. Ruani, et. al., Sol. En. Mater. Sol. Cells, **92**, 537 (2008).

1. Introduction.

Dye-sensitized solar cells (DSSCs) represent a low-cost candidates to substitute the silicon-based conventional photovoltaic devices, and exhibit with a liquid electrolyte, a high conversion efficiency of the solar radiation (>11%) . The presence of a liquid electrolyte, with the redox couple I_3^-/I^- , in DSSCs constitutes a strong limit to the use and mass production of this kind of device, because of sealing and handling problems. For this reason, most of the research activities in this field in recent years have been devoted to the substitution of the liquid electrolyte with either solid-state ionic conductors (gel and polymer electrolytes) or solid-state hole conducting materials. The solid-state DSSCs consist of a few microns thick mesoporous TiO_2 film grown on a transparent electrode, the mesoporous film is decorated with a monolayer of dye and than infiltrated by a suitable hole conducting material (HCM) that fills the empty pores and on top of which the second metallic electrode is deposited. The possibility to tailor organic components, like HCM, could give, in principle, a higher conversion efficiency with respect to the classical liquid electrolyte, by choosing those with the more appropriate HOMO-LUMO levels. Thanks to the intensive efforts in trying to obtain high efficiency solid-state dye-sensitized solar cells, their performances have been strongly improved since a few tenths of percent to a maximum of about 4% . This result is still far from the 11% efficiency obtained in liquid electrolytic DSSCs.

The electron transfer dynamics from dye to TiO_2 and electron-hole recombination constitutes the major limiting factor of the power conversion efficiency of a cell. In particular, to reduce electron-hole recombination in the dye site one should either introduce a barrier to reduce back electron transfer or improve the fast collection of the two kind of carriers at the two electrodes. It has been shown that the major problem is related

to obtaining of a very large intimate contact through all the depth of the device among the TiO_2 mesoporous layer and the solid-state hole conductor . The “limited” efficiency in solid-state DSSCs (4%) is the result of a compromise between the difficulty to efficiently infiltrate the HCM more than one or two micron thick mesoporous titania films and the necessity to have larger mesoporous TiO_2 thickness ($\sim 10\mu\text{m}$), and consequently a sufficient amount of dye, in order to absorb efficiently the incident light. To overcome this problem different routes have been pursued like in situ polymerization of the hole conductor and ordered self organized structures that could favour either the infiltration of the HCM or the light harvesting process .

In a previous paper, some of us have shown that inverse opal (IO) titania films can act as easily impregnable large surface structures to be used in solid-state dye-sensitized cells. Relevant efficiency increases, using IO titania films have been shown also for CdSe quantum-dot-sensitized TiO_2 solar cells . The fabrication procedures for IO mesoporous films, followed up to now, is multi steps and time consuming. First, the opal-like templating film formed by the polystyrene (PS) beads is deposited on the substrate, this process is quite slow because it is determined by the evaporation of the water/beads solution where the substrate is partially immersed. Once the opal film is formed it is consolidated by annealing it around the glassy temperature of the PS and than infiltrated with the TiO_2 precursor. The substrate is now ready to be heated in order to remove the templating PS and transform the precursor into TiO_2 . This process is strongly time consuming and consequently, despite the advantages of using IO in fabrication of solid-state dye-sensitized solar cells, makes it not applicable in any possible mass production of DSSCs. Here, we successfully tested, whether it was possible to obtain mesoporous films of titania, showing large domains of IO structures, using fast coating systems like the doctor blade technique. With this aim, water solutions of PS beads and TiO_2 precursor at different relative concentrations have been used. A similar procedure have been recently discussed

by Qi et al. . We have observed that a single phase IO structure formed by interconnected ordered cavities could be achieved only in the case the titania precursor in the solution was not exceeding a minimum amount needed for coating, in a single monolayer, the PS beads.

2. Experimental

Monodispersed PS spheres are prepared by surfactant-free emulsion polymerization of styrene, as described in detail elsewhere . The water suspension of polystyrene beads and titanium (IV) bis(ammonium lactato)-dihydroxide (since now on indicated as Ti-Lactate) was obtained by mixing a water suspension of PS (2.13 vol % - indicated as H₂O/PS) and water solution of Ti-Lactate (50 wt% from Aldrich – indicated as H₂O/Ti-Lactate). All the water solutions discussed in this paper have been prepared using 270 nm diameter PS beads.

The initial solution has been prepared starting from the hypothesis that no more than 50% of the interstitial space leaved empty by the PS spheres in a FCC structure and that the templating part, constituted by the self-assembled PS, occupies 74% of the total volume. Considering that 23.1 ml of H₂O/Ti-Lactate corresponds to 1 cm³ of bulk TiO₂, the relative amount of H₂O/PS and H₂O/Ti-Lactate that satisfy the geometrical condition previously indicated are give by 1 ml of H₂O/PS and 0.064 ml of H₂O/Ti-Lactate. This correspond to a 1.71 g of Ti-Lactate per 1 g of PS . This solution, used as the reference one, is labelled as SOL100, all the other solutions are labelled SOLxx where xx indicates the PS/Ti-Lactate ratio, normalised to 100 relative to the concentration of SOL100. Films were obtained by dropping and spreading SOLxx using a blade on a glass substrate and dried out. The samples were than heated in a furnace to 500 °C (1.6 °C/min) in air and kept at this temperature 1 h, then cooled in 5 h to room temperature – all the samples discussed in

this paper have been exposed to the same heat treatment cycles. Films of different thickness (0.5 - 7 μm) have been investigated without observing any dependence on it.

SEM images are obtained using a Zeiss FEG-SEM LEO 1530 electronic microscope. In order to avoid image distortions due to electrostatic effects, before SEM observation, the TiO_2 films were gold coated. The gold films of about 15 nm were deposited by argon sputtering.

Raman scattering measurements are performed in back-scattering geometry using a Renishaw 1000 micro-Raman instrument equipped with a charge-coupled device CCD camera and microscope lenses with x100 and x50 magnification. The excitation was provided by the 514.5 nm line of an Ar^+ laser. The near-infrared (NIR) excited Raman scattering measurements were performed in a back-scattering configuration by means of a RFS 100 Bruker Raman interferometer. A diode pumped c.w. Nd:YAG laser was used for excitation with $\lambda_{\text{ex}} = 1064 \text{ nm}$, with a laser spot of approximately 0.3 mm in diameter. The scattered radiation was detected by a liquid nitrogen cooled Ge detector in a wide spectral range, from 80 up to 3500 cm^{-1} in the Stokes side and from 150 up to 1000 cm^{-1} in the anti-Stokes side. In both micro-Raman and NIR excited Raman the resolution was 1.0 cm^{-1} and the accuracy better than 0.5 cm^{-1} .

3. Results and discussions.

As already mentioned (see Experimental paragraph), the former solution – labelled SOL100 – has been prepared estimating the relative amount of PS and Ti-Lactate taking into account that the empty space of a faced-centred cubic (FCC) closed-packed structure (the one that will constitute the IO) is about 26% by volume and that, because of the intrinsic nanoporosity of the final inverse opal TiO_2 skeleton, no more than 50% of the empty space will be filled. ~~The SOL100 was dropped and spread using a blade on a glass~~

~~substrate and dried out. The sample was then heated in a furnace to 500 °C (1.6 °C/min) in air and kept at this temperature 1 h, then cooled in 5 h to room temperature — all the samples discussed in this paper have been exposed to the same heat treatment cycles.~~

Raman scattering has been demonstrated to be a fast and excellent tools to characterise materials. Raman allows to determine the presence of possible different phases (e.g. anatase and rutile for TiO₂) and of impurities like carbon residuals and also the degree of crystallinity of a system. It has been shown that linewidths (Γ_i) and peak positions (ω_i) of the two E_g Raman modes around 145 and 635 cm⁻¹ (indicate as 1 and 4 respectively) of TiO₂ lactate can be used as good parameters for characterising the dimensions of the titania crystallites (see figures 3 and 4 in Ref.).

The Raman investigation of the titania films obtained using the SOL100 shows that anatase is the only crystalline phase detectable (same conclusions have been obtained for the titania film examined in this paper). The two E_g Raman modes can be fitted using Lorentzian curves; the energies (ω_i) and half linewidths (Γ_i) of the two modes are $\Gamma_1 = 15.4$ cm⁻¹, $\omega_1 = 147.8$ cm⁻¹ and $\Gamma_4 = 31.3$ cm⁻¹, $\omega_4 = 642.6$ cm⁻¹ respectively. These values are compatible with crystalline anatase domains of about 10 nm. The images taken with the Scanning Electron Microscope (SEM) show that the deposited material is forming a strong non-homogeneous film composed of compact grains of various diameters ranging from about 50 nm up to a few microns that are partially covered by an nearly ordered inverse opal layer (see Fig. 1). The IO constitutes a negligible portion of the titania film. The pore diameters of the IO are about 185-190 nm; that means a contraction of about 2/3 with respect to the initial volume of the templating PS beads, whose diameter was 270 nm.

In order to obtain a mesoporous titania film free from the bulky component observed in the case of SOL100, the H₂O/Ti relative concentration was reduced to 1/3 (SOL33) in order to

compensate for the large volume contraction observed after the heat treatment. Both SEM observation and Raman scattering of SOL33 provided similar results as those obtained in the case of SOL 100. This indicates that the filling of the interstitial space is much smaller than the hypothetical occupation of 50%. The relative Ti-Lactate concentration in the solution has been reduced continuously, as to obtain the complete disappearance of the bulky TiO₂ component.

Inverse opal titania films free of the bulky TiO₂ component are observed only when the Ti-Lactate relative concentration in the solution is equal or smaller than 1/10 of the initial one (SOL100), that corresponds to 1 ml of H₂O/PS and 0.006 ml of H₂O/Ti-Lactate (SOL10). SEM images show quite large IO ordered structures (Fig. 2 and Fig. 3), the ordered pores are interconnected through the holes at the boundary between adjacent spheres. The presence of three holes at the bottom of each pore is coherent with the close-packed structure that is usually obtained exploiting the self-organisation properties of monodispersed PS beads . The apparent thickness of the walls of the IO structure in Fig. 3 is not intrinsic but is probably related to the gold coating film that was deposited on top of the sample in order to avoid electrostatic effects. In Fig. 4 the Raman spectra of the films obtained using SOL10 and SOL100 are presented. Because the cut-off edge of the holographic filter, used in the micro-Raman system in the case of the 514.5 nm excitation laser, does not allow to detect scattered light with a difference in energy of about 200 cm⁻¹ with respect to the excitation, we used the NIR Raman set-up to observe the E_g Raman mode of TiO₂ around 145 cm⁻¹. On the other hand, the Raman scattering cross section at $\lambda_{\text{ex}} = 1064 \text{ nm}$ is very small, consequently, only the most intense Raman mode of titania could be detected during the investigation of mesoporous titania thin films also accumulating for each sample more than 20,000 scans of the interferometer. As a consequence, the Raman spectra are presented as a sum of two different contributions in the two separate ranges (see Fig 5), the relative intensities of the features in the right and

in the left side of the figure are arbitrarily assigned. The fitting parameters for the two E_g Raman modes for the SOL10 film are $\Gamma_1 = 17.2 \text{ cm}^{-1}$, $\omega_1 = 148.1 \text{ cm}^{-1}$ and $\Gamma_4 = 37.2 \text{ cm}^{-1}$, $\omega_4 = 642.6 \text{ cm}^{-1}$. These values give a mean dimension of anatase crystallites of the order of 7-8 nm. Despite the fact that the calcination process followed for all the films was the same, we observe a reduction of the mean crystallite dimension of the TiO_2 mesoporous film obtained from SOL10 with respect to those of the films prepared from solutions using the higher relative Ti-Lactate concentrations. This is consistent with the absence of compact grains in the titania films obtained using SOL10. ~~In fact, in SOL10, the growth of the crystallite dimensions is inhibited by the absence of adjacent large amount of TiO_2 .~~

The small amount of TiO_2 precursor in the solution for SOL10 corresponds to a very low filling of the available interstitial space of the closed-packed structure of about 20% and not the expected 50%.

This is due to the fact that there is not really an interpenetration of the two components of the solution during the drying process of the film when the beads self assemble to form the template opal structure. Only those molecules that are either adsorbed on the surface of the beads or those that are randomly trapped in the interstitial sites of aggregated beads will contribute to the formation of the IO structure. We can then exclude a two steps process where beads precipitate self assemble forming the template structure and in a second step the Ti-Lactate diffuses inside this structure filling the voids. A qualitative estimation obtained by considering the dimension of the available PS surface and the number of Ti-Lactate molecules in solution is suggesting that approximately one Ti-Lactate molecule per two phenyl rings of the PS is adsorbed at the beads surface. This ratio is easily obtained by calculating the mean Ti-Lactate/Ti-Lactate distance assuming that in the case of the optimised solution, SOL10, all the Ti-Lactate molecules are adsorbed at the

surface of the PS beads. The same result of approximately one Ti-Lactate molecule per two phenyl rings on the PS surface is obtained by considering the steric hindrance of the materials in ~~exam~~ under consideration (see Fig. 5). The Ti-Lactate molecules in water solution are driven by hydrophobic attraction forces to be adsorbed on the PS beads whose surface is formed by phenyl rings. The process continues up to the full coverage of the surface. In solutions, like the one indicated as SOL100, where the amount of Ti-Lactate is in excess with respect to the optimised ratio only a small part of the Ti-Lactate that is not absorbed at the PS surface could infiltrates within the closed-packed structure during the ~~desiccation~~ drying process of the solution on the substrate. Most of excess Ti-Lactate precipitates when the solution reaches saturation during the desiccation process before the PS beads start to aggregate forming the IO, in fact, as is observed in figure 1, the ordered mesoporous structure in these films appear as a superimposed layer on top of the bulky structure.

5. Conclusions

We have obtained mesoporous nanocrystalline titania films showing inverse opal structure by using a fast, simple, one step method, like doctor blading. The hydrophobic attraction ~~forces~~ among the Ti-Lactate molecules and phenyl rings on PS beads surface in aqueous solution determines the ~~blanket~~ coating of the PS beads before these starts to aggregate forming the template structure of the film while the solution is drying. A thermal treatment results in a IO structured film whose final cavities are about 180 nm in diameter and appear interconnected through holes of about 50 nm. The titania IO structure, because of its three dimensional ordered open structure, is intrinsically easy impregnable; it has already been shown that the use of such a 3D structure in all solid-state dye sensitized cells strongly improves the efficiency of these devices. The simplicity of this approach

could represent the keystone for allowing mass production of efficient solid-state dye sensitized solar cells.

Acknowledgements:

We would like to thank Prof. Hristina Spasevska for helpful discussions. Partial support from the Centro Ceramico di Bologna and CECERBENCH laboratory are kindly acknowledged.

FIGURE CAPTIONS

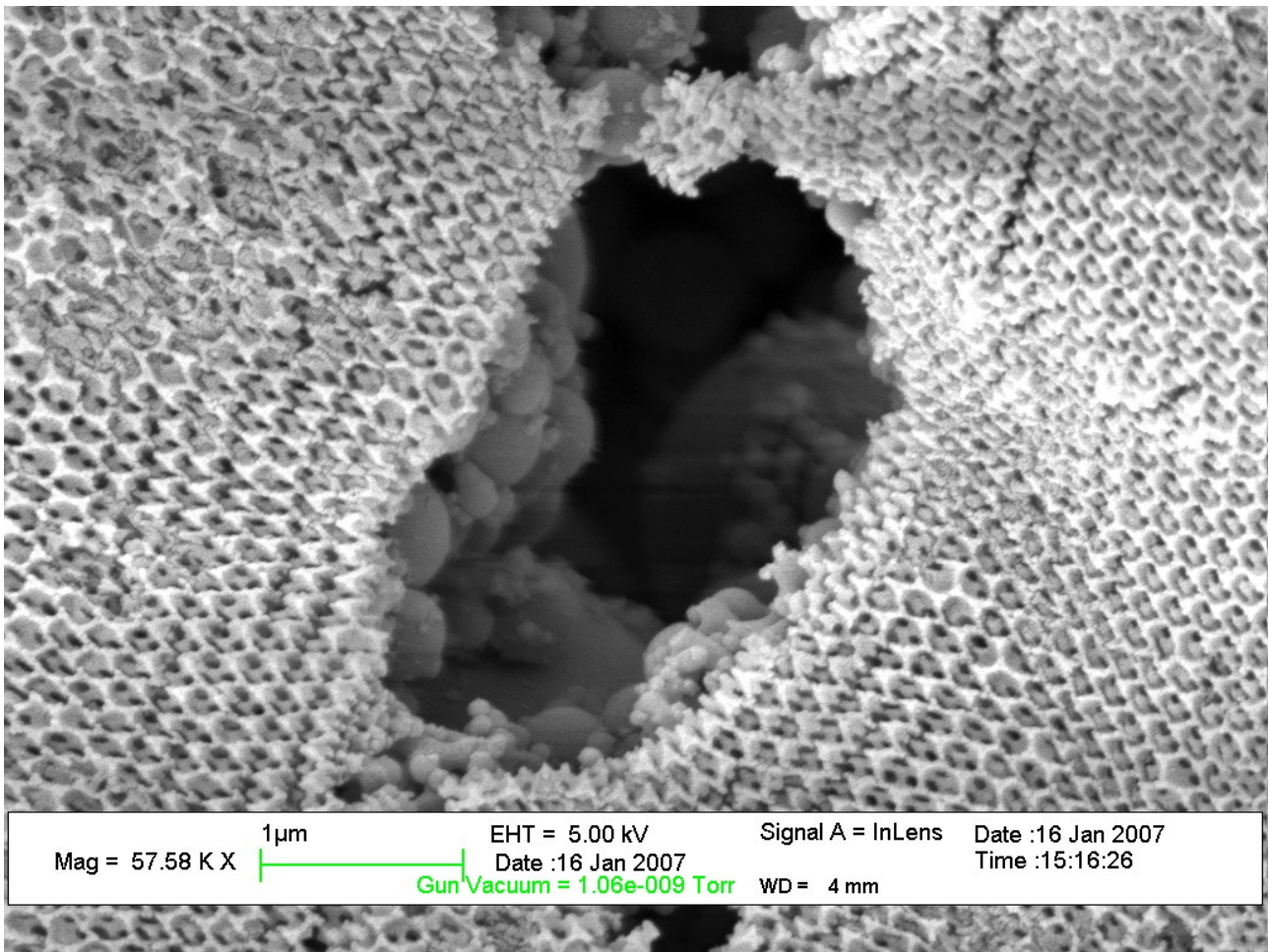


Figure 1. SEM image of a portion of a TiO₂ film obtained using SOL100; a thin IO layer is partially covering bulky TiO₂ grains; the interconnection among different planes of the IO structure is clearly observable in the image as black dots in the bottom of the honeycomb structure.

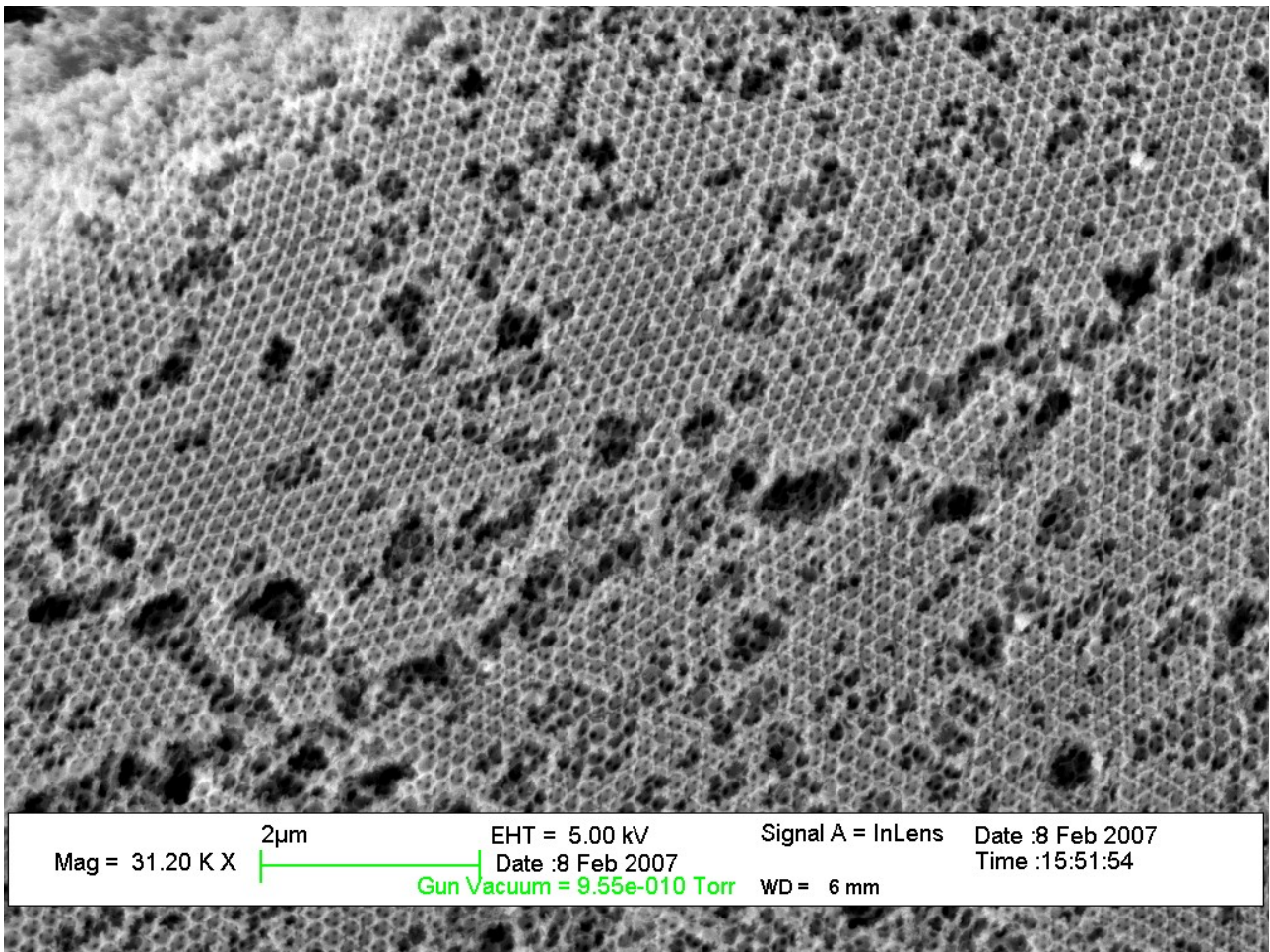


Figure 2. SEM image of a part of a TiO₂ film obtained using SOL10; large domains of IO titania obtained in a one step deposition by doctor blading are visible.

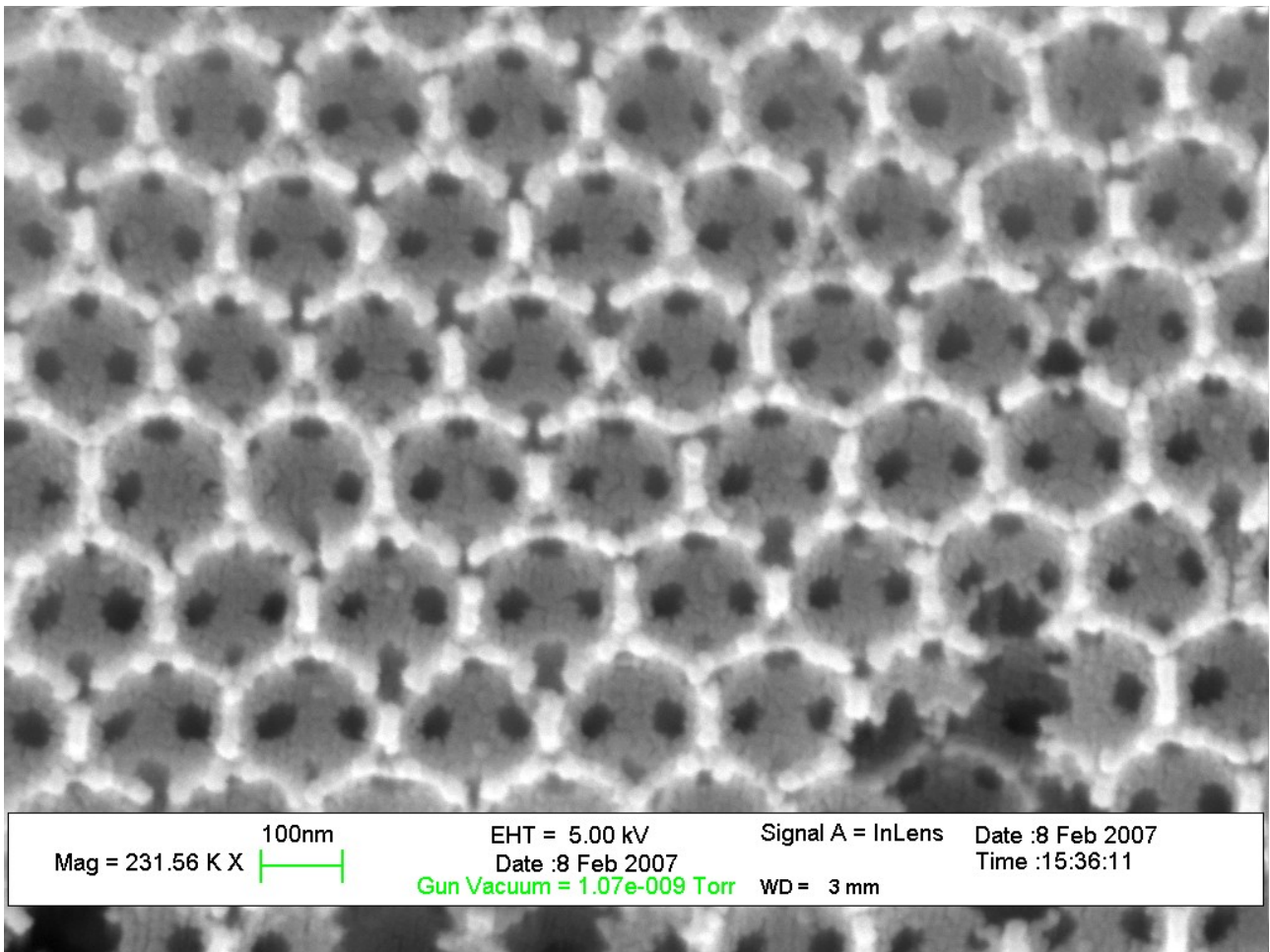


Figure 3. SEM image of a portion of TiO₂ film obtained by the doctor blade technique using SOL10; the interconnection among different planes of the IO structure appears as black dots of approximately 50 nm.

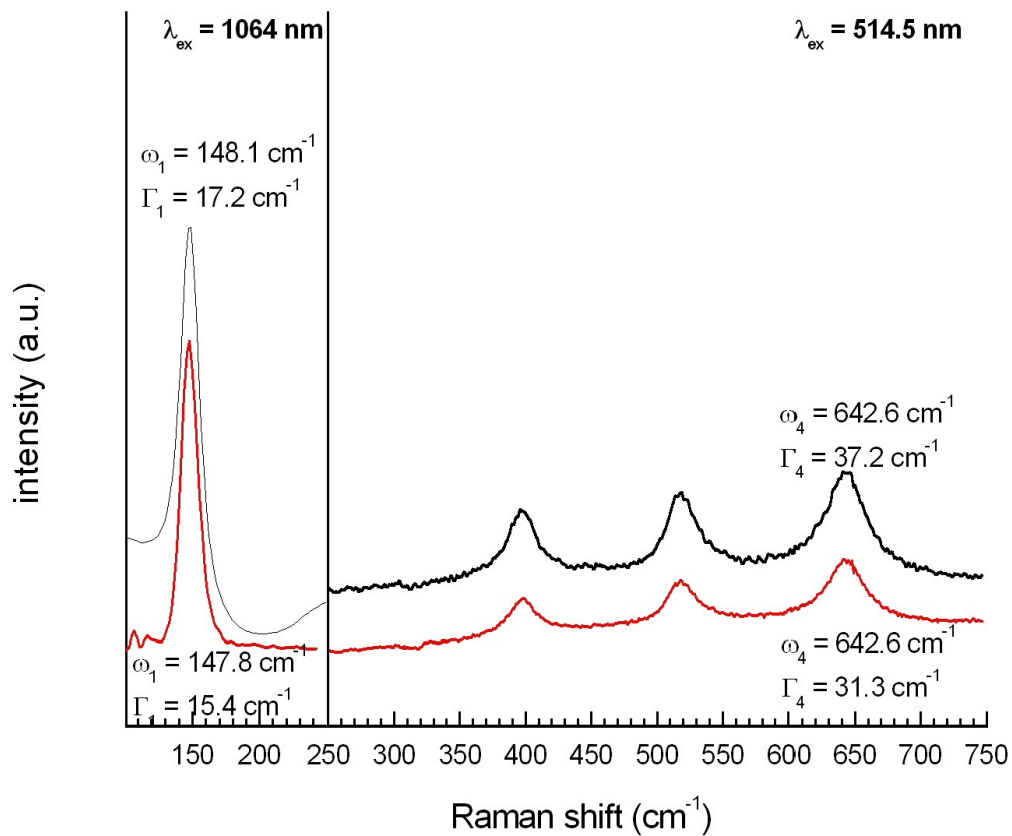


Figure 4. Raman spectra of a titania films obtained by the doctor blade technique by using SOL100 and SOL10. The low energy side of the spectra has been obtained exciting at 1064 nm using a NIR Raman set-up (Bruker RFS 100); the high energy side has been collected exciting at 514.5 nm with a micro-Raman Renishaw 1000. Both spectra are typical of the anatase phase of TiO_2 , no other phase is detectable. The halfwidth and energy position analysis of two of the active Raman modes – around 145 and 640 cm^{-1} – shows a difference in the microcrystallites size distribution for the two samples. The relative Raman intensities of the left and right sides of the spectrum are arbitrarily given.

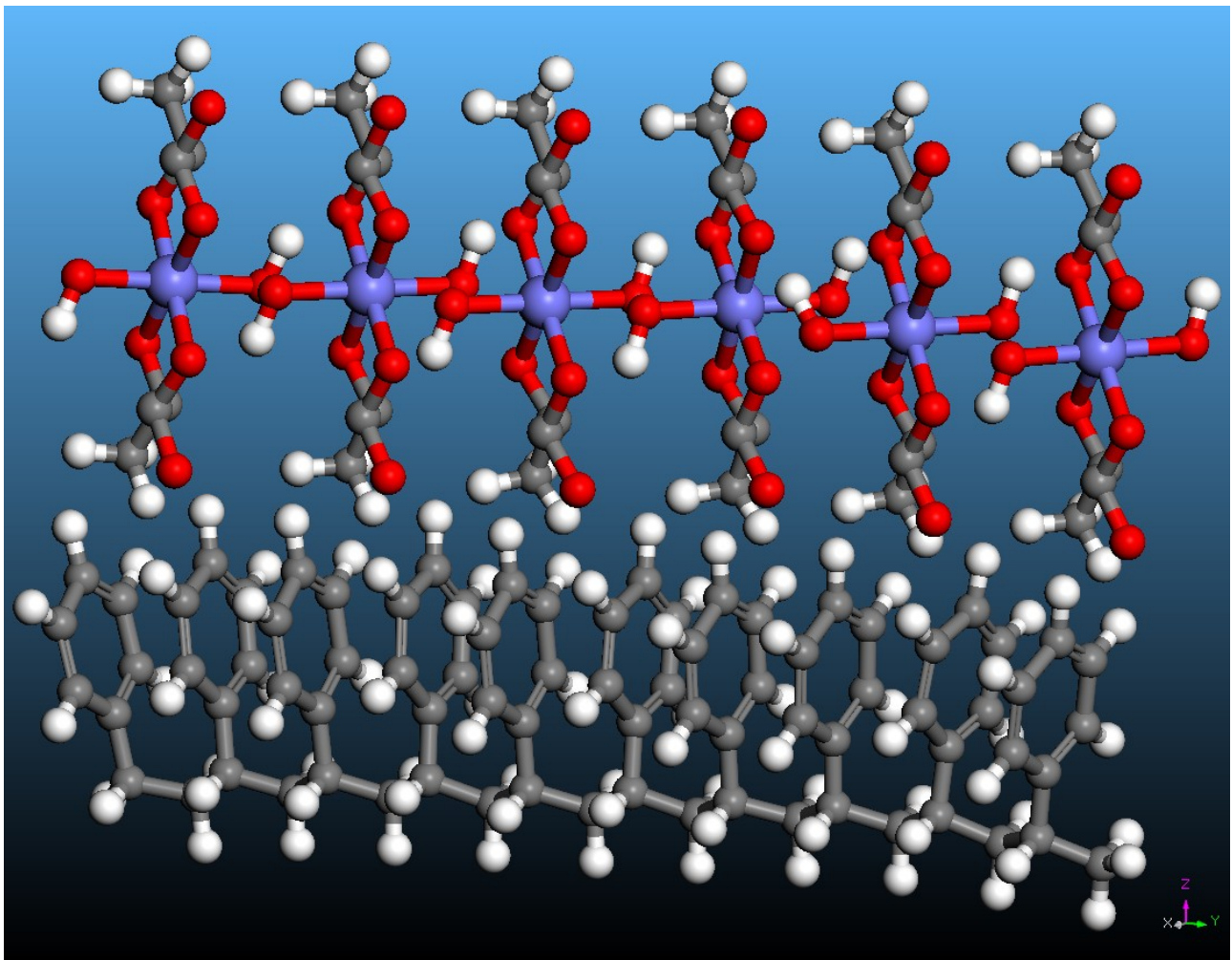


Figure 5. The figure represents a projection of the arrangement of Ti-Lactate - approximately to one molecule per two phenyl rings - at the surface of the PS beads. A 2D expansion of this arrangement corresponds to a close package of Ti-Lactate molecule in the plane. The figure has been drawn using Materials Visualizer by Accelrys.